BNL-103667-2014-TECH

AGS/RHIC/SN 041;BNL-103667-2014-IR

Field Map Generated Matrices for Spin Tracking

A. Luccio

November 1996

Collider Accelerator Department

Brookhaven National Laboratory

U.S. Department of Energy

USDOE Office of Science (SC)

DISCLAIMER

Alternating Gradient Synchrotron Department
Relativistic Heavy Ion Collider Project
BROOKHAVEN NATIONAL LABORATORY
Upton, New York 11973

Spin Note

AGS/RHIC/SN No. 041

Field Map Generated Matrices for Spin Tracking

Alfredo U. Luccio

November 5, 1996

FIELD MAP GENERATED MATRICES FOR SPIN TRACKING *

ALFREDO U. LUCCIO †
RIKEN Institute, Wako, Saitama, 351-01, Japan

1. Introduction

Spin tracking in RHIC tries to answer the very basic question whether the spin polarization of the proton will be conserved up to the highest energies with the help of Siberian snakes. In a first stage of the numerical tracking, an analytical expression for the orbit and spin matrices in the snakes was used. We are now moving to the use of matrices calculated by a more realistic description of the magnetic field in the snakes. This task presents several problems, both for orbit and for spin matrices. We are proceeding in successive steps of approximation. Let us discuss what the steps are and what we expect to accomplish.

The limits of this study are the following. For the orbit we will use a zero order matrix. That is, the coefficients of the transformation of the spatial phase space coordinates will be constants, independent of the position and angle, in six dimensions, of the particle. For the spin, instead, we will use in the snakes 3×3 matrices whose elements are a function of the particle position. Spin motion will be then treated to first order, but it will couple with the orbital motion.

Spin matrix elements dependence on the orbit is particularly important at the highest limit of the energy in RHIC, since there spin resonances are strong and overlapping and the capability of the snakes to preserve proton polarization is limited. This in turn presents us with two main problems, on the optimization of the spin matrices and of the orbit matrices for the snakes.

=> Numerical spin matrices should be unitary, since they represent a rotation in spin space, but also they should provide the required rotation of the spin and the correct angle of the precession axis. To achieve that, the snake magnetic field should be varied along the acceleration cycle. Then, spin matrix elements are also a function of the energy.

=> Orbit matrices should be symplectic, essentially to preserve beam emittance, among other motion integrals. If the emittance blows up during tracking, particles will end up on the average on large radii, and then the spin matrices will show an incorrect rotation of the spin. Since in spin tracking a large number of revolution should be simulated, we can only tolerate a small error in symplecticity.

In the following we show how to generate from a magnetic field map consistent spin and orbit matrices, to be used in spin tracking

2. Use of Field Maps

Our spin tracking program *Spink* [1] makes use of two type of matrices: 6×6 Orbit matrices (T), and 3×3 spin matrices (S). In RHIC, snakes and spin rotators are made

*Work performed under the RIKEN Eminent Scientist Invitation Program
†Permanent address: Brookhaven National Laboratory, Upton, NY 11973-5000, USA

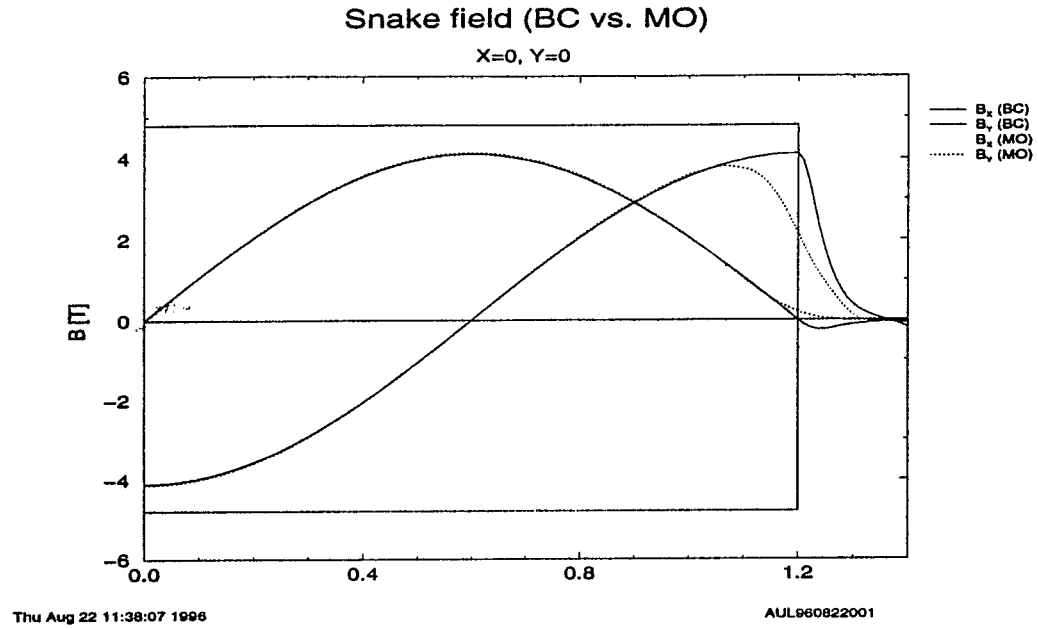

Figure 1: Snake field. BC vs MO. On axis.

with four helices [2].

In an earlier use of the analytical representation of the snake field given by Blewett-Chasman (BC) [3], explicit expressions for T matrices [4] and S matrices [5] had been calculated to first order in the field. For a better representation of the real snakes/rotators, the analytical formulation is not sufficiently accurate, and the BC field should be replaced by a field map calculated by some three dimensional magnetic field calculation [7] or measured. A map of the field of the slotted-type helix presently being constructed at Brookhaven [8] was calculated on a (x, y, z) mesh [9]. The results presented in this note are based on this map (MO map),

We first compared the field on the MO map with the BC field used in earlier version of *Spink* and in the optimization of the snakes/rotators [1]. Figures 1 and 2 show the results of the comparison. It is apparent from the figures that the field integral of the MO field is somewhat smaller than for the BC field, for the same nominal (maximum) field, because the magnetic component that has a maximum close to the magnet's end is smaller due to the fall-off of the field towards the outside.

The integration of the equation of motion and of the spin (BMT) equation in the MO map has shown that the appropriate rotation of the spin in a snake, 180^0, and the correct angle of the precession axis, 45^0, is obtained with a substantially higher peak field (1.290 and 4.185 tesla, in the outer and inner helices respectively, vs. 1.191 and 3.864 tesla for the BC field, at a beam energy $\gamma = 27$). This is a reason for concern and points out how important it is to switch to a correct characterization of the snakes/rotators, by using maps and not an analytical representation of the field.

A second task was to include in the S matrices effects due to the betatron motion, that according to some calculations [11] seem to reduce the snake power especially at

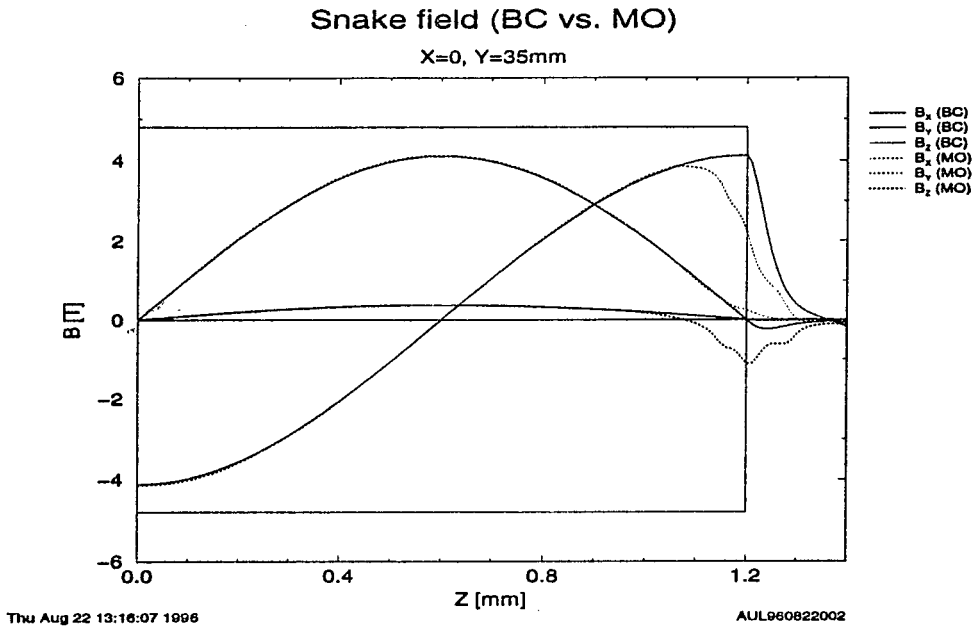

Figure 2: Snake field. BC vs MO. Off axis.

high energy in RHIC. Betatron motion affects S matrices because the local field on the particle orbits is slightly different than the nominal field at which the matrices can be optimized. Then, the elements of the S matrices for a snake should be made a function of the particle transverse position, similarly to what happens in other lattice devices, like quadrupoles. Analytical (Syphers) matrices already include this effect, since their elements are a function of the (local) magnetic field, that can be derived from the BC expressions. Now, we want to include the effect in matrices calculated from a magnetic field map.

T matrices should also contain effects due to the field calculated on the orbit. Analytical (Courant) orbit matrices contain this dependence, since their elements are expressed in terms of the (local) orbit curvature, proportional to the local magnetic field. For T matrices we also want to use an expression calculated from a magnetic field map.

3. Spin Matrix Calculation From a Field Map

To calculate a S matrix from the MO map we used the integrator *Snig* [10]. The field was mapped on a cartesian grid with 5 mm step in the transverse (x, y), and 10 mm step in the longitudinal z direction. The interpolation in the field was done with a cubic polynomial in 3 dimensions on a mesh of 3^3 field points. Calculations were done in double precision. The map was used four times, for the four helices of the snake, with the appropriate orientation of the field at each helix entrance.

Three representative particles were injected in the field, with initial spin $\vec{S} = (1,0,0),(0,1,0)$ and $(0,0,1)$, respectively. With this initialization, the final values

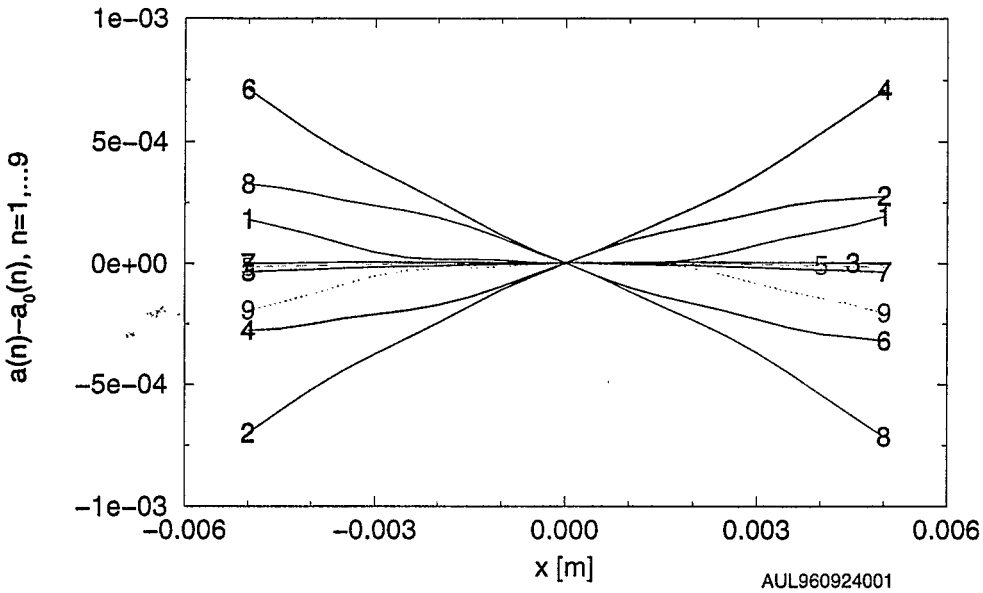

Figure 3: Snake S matrix coefficients vs. x. MO map. $\gamma = 27$

of the three components of the spin give directly the elements of the S matrix. To study the dependence of the matrix elements from the particle position and angle, the calculation was repeated for different values of $\vec{X} = (x, x', y, y')$. The determinant of each matrix, for different points $\vec{X}$, resulted very close to one with an error of the order of 10^{-14}.

The values of the matrix elements for the snake, 1 to 9 row-wise, as a function of (x, x', y, y') are shown in figures 3, 4, 5, and 6, respectively. They appear rather smooth up to large values of x and y that correspond to orbits actually reaching the outer edges of the field map, and represent unrealistic large betatron oscillations in RHIC. We performed a quadratic polynomial χ^2 fit of the matrix elements vs. the components of $\vec{X}$. Figures 7, 8, 9, and 10 show the result of the fit, and the corresponding values of the matrix determinant error $(det(S) - 1)$. The determinant error was always less than 10^{-6}. Finally, we combined our results in a quadratic expansion of the spin matrix elements in all components of $\vec{X}$. No cross terms were included in the expansion. Fitting routines came from the Numerical Recipes [12].

The resulting $9 \times 5 \times 2$ numbers that characterize a spin matrix for a MO map of the snake are shown in Table I. The table gives the coefficients of the following expression for each of the matrix elements, 1 to 9, arranged row-wise

$$a = a_0 + A\,x + B\,x' + C\,y + D\,y' + E\,x^2 + F\,x'^2 + G\,y^2 + H\,y'^2 \qquad (1)$$

We checked the expression and the numbers, by calculating the matrix on a large 4×4 mesh of $\vec{X}$ points. The determinant maximum error over the mesh resulted of the order of 10^{-6}.

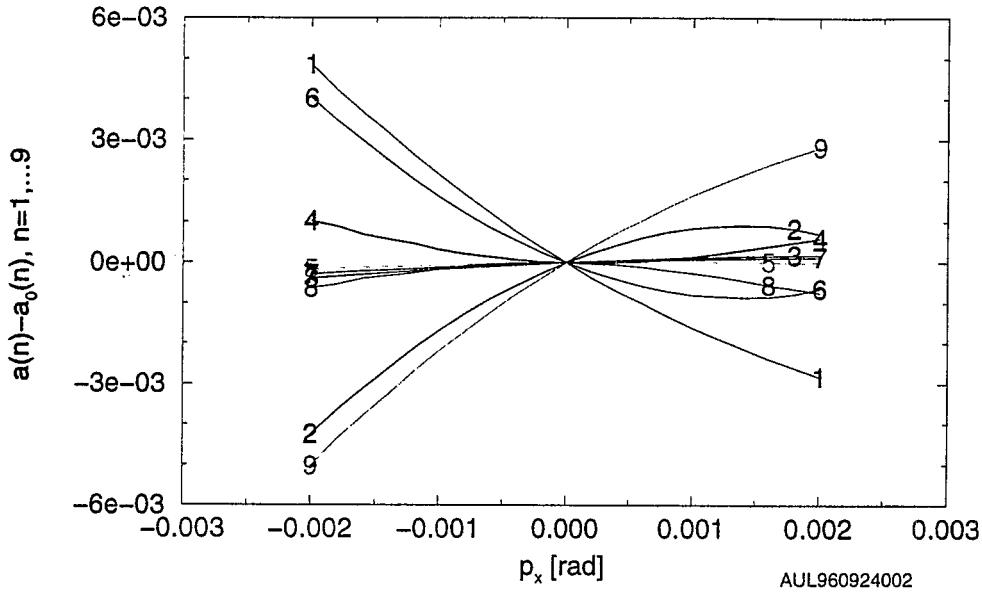

Figure 4: Snake S matrix coefficients vs. x'. MO map.

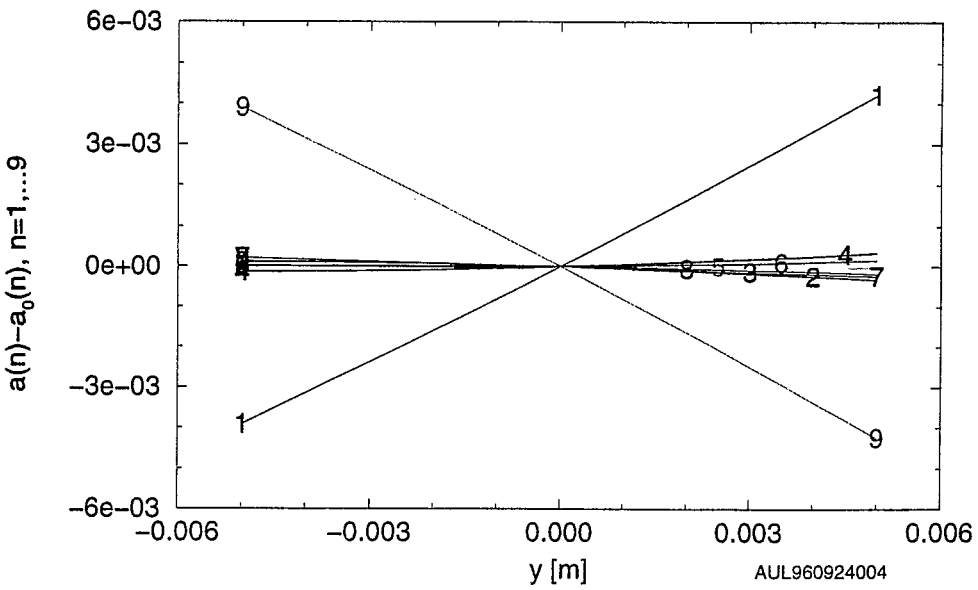

Figure 5: Snake S matrix coefficients vs. y. MO map.

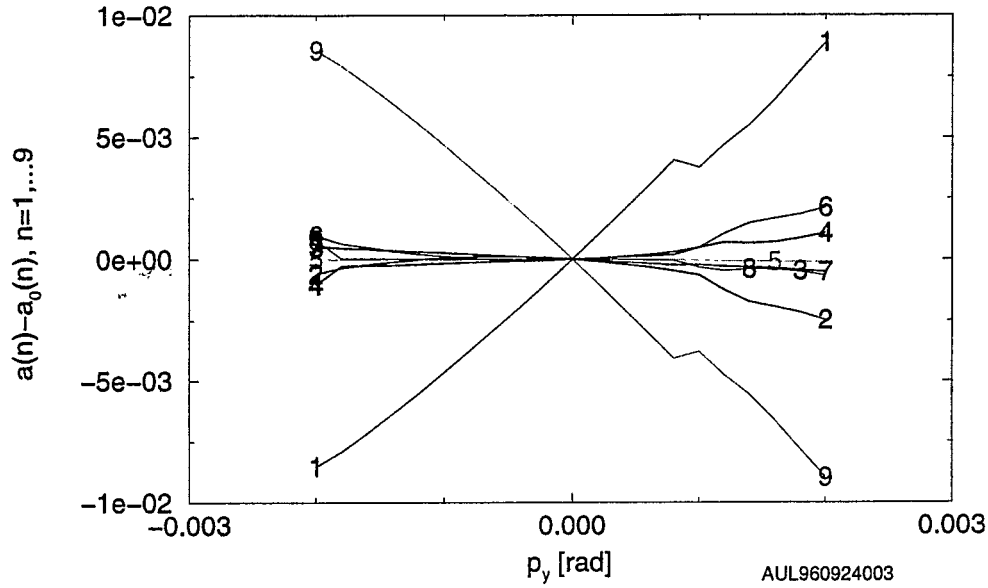

Figure 6: Snake S matrix coefficients vs. y'. MO map.

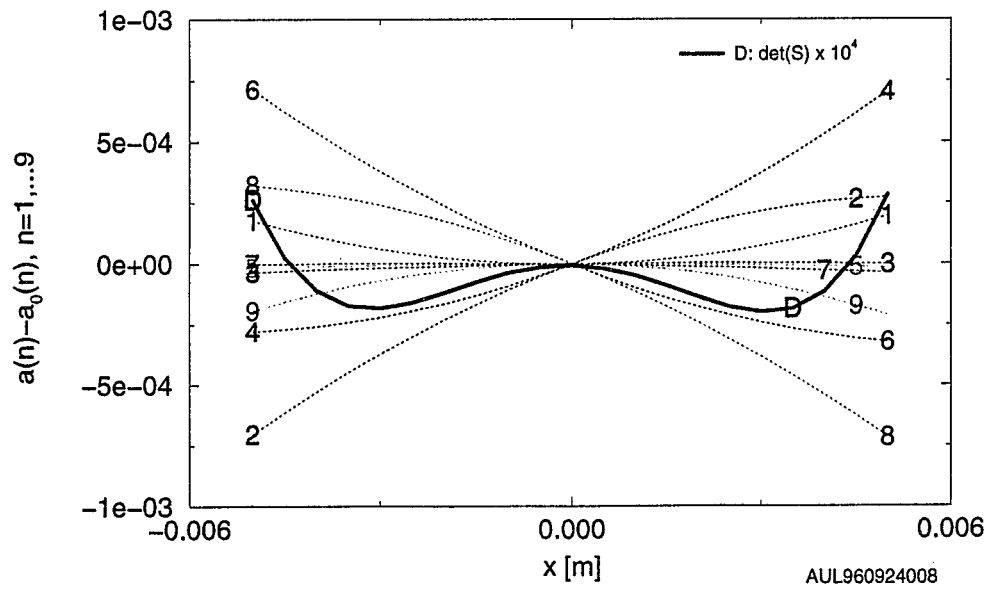

Figure 7: Snake S matrix coefficients vs. x. Quadratic fit.

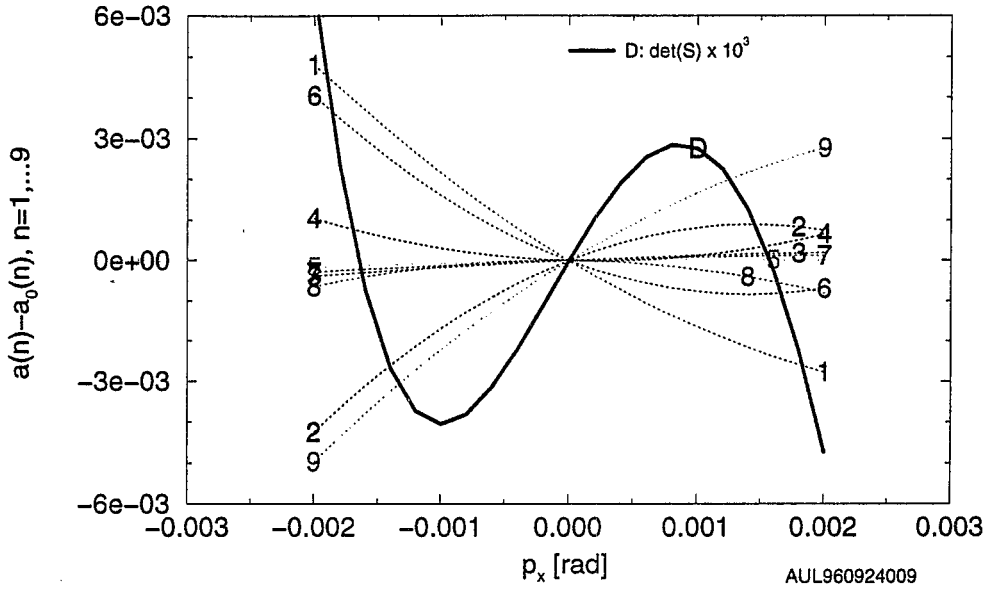

Figure 8: Snake S matrix coefficients vs. x'. MO map. Quadratic fit.

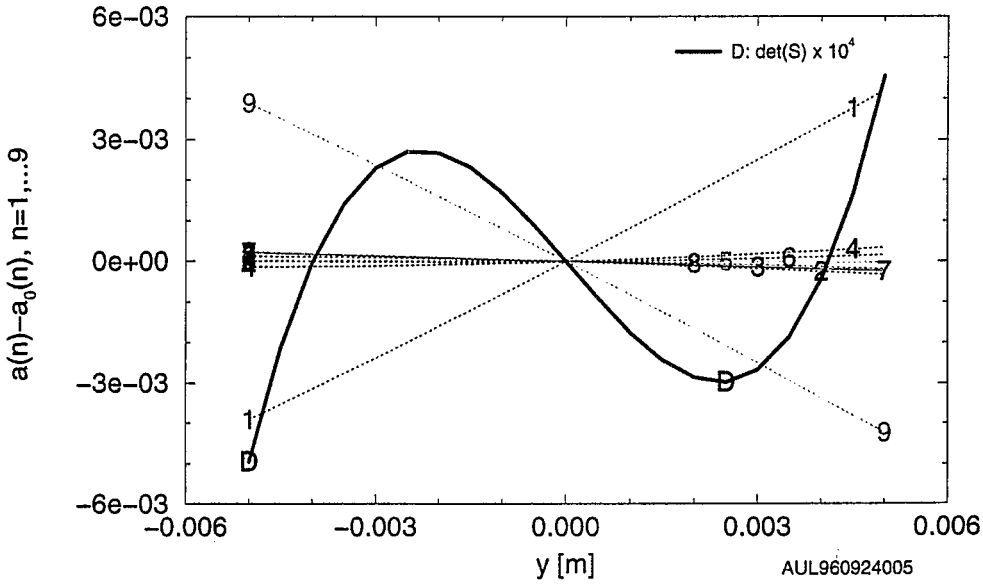

Figure 9: Snake S matrix coefficients vs. y. MO map. Quadratic fit.

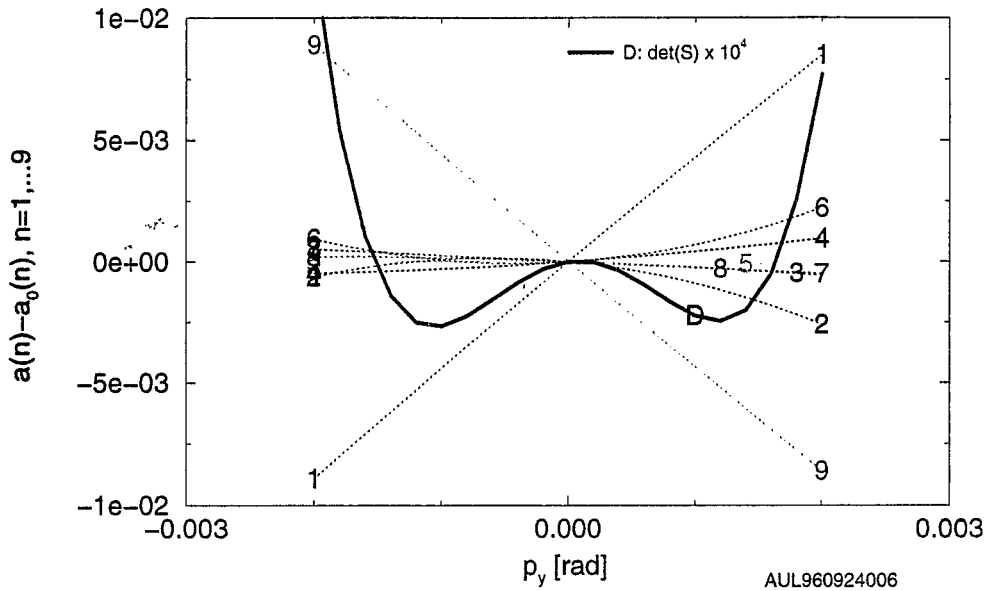

Figure 10: Snake S matrix coefficients vs. y'. MO map. Quadratic fit.

Table I: Snake S Matrix. Coefficients of the expansion in (x, x', y, y').

a_0	A	B	C	D
-5.4130701775829029E-2	1.8160520224 96E-3	-1.89495956849	0.811944208831	4.35162079850
3.5405617524792550E-2	9.771986548074E-2	1.24911320560	-4.525811813585E-2	-0.490790835740
-0.9979056574833112	3.360358963308E-3	0.144291475643	-4.543676535538E-2	-0.253245262471
-3.5367726899755189E-2	9.823043608381E-2	-9.547229506081E-2	4.846007606141E-2	0.366648436509
-0.9988107748848698	-2.119156011162E-5	4.158788181623E-2	-2.216440119416E-3	-2.342376038373E-2
-3.3527622605374612E-2	-0.103344099216	-1.18282407037	1.407227377854E-2	0.321660792845
-0.9979073058766534	-3.565845902588E-3	0.104838207564	-4.567401192705E-2	-0.249597986451
3.3518332775825485E-2	-0.103843330131	-3.779493119458E-2	-1.836433192659E-2	-0.195767578472
5.5319051041207323E-2	-1.778565792294E-3	1.93523382914	-0.812776774999	-4.37231011746
	E	F	G	H
	7.49874342184	254.296215912	6.21405438357	-54.3392714027
	-8.59619188986	-437.720837433	-4.01090495982	-398.090585500
	-0.705485225718	-26.4058528541	-0.173881822919	-1.51033866261
	8.56693476956	210.884397821	4.29413521716	64.0535181173
	-0.557101922817	-20.5128387403	-0.271080679991	-15.2650066526
	7.87715154291	417.871846144	3.84644588563	399.781046205
	-0.704252483781	-19.2741745797	-0.155576224717	10.2193866972
	-7.86300110507	-182.580251919	-3.88526513592	-46.5634105139
	-8.07080440953	-277.079651666	-6.81824485907	37.3891140337

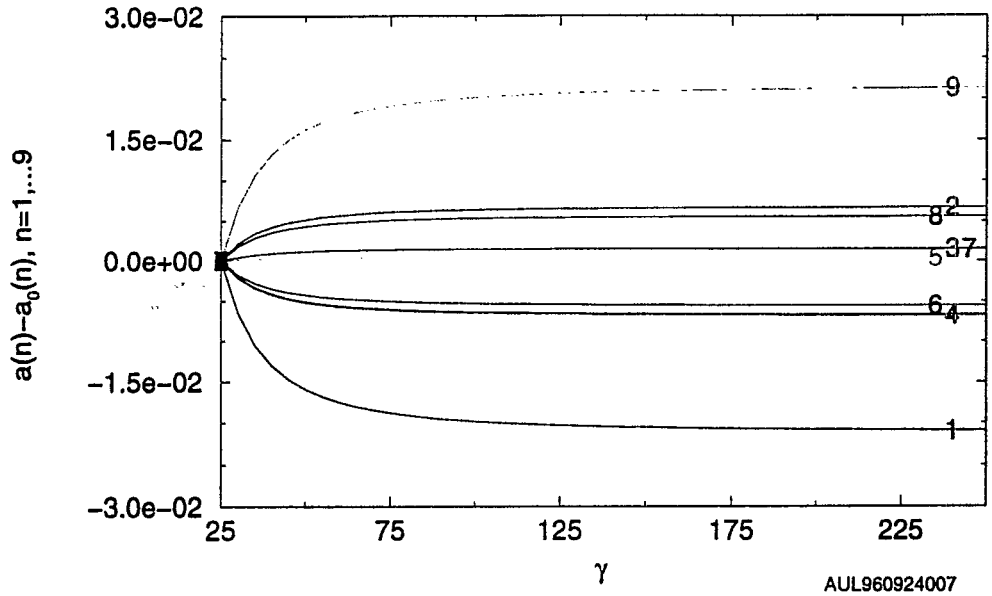

Figure 11: Snake S matrix coefficients vs. γ. MO map

For optimum performance, the magnetic field in the snake should be adjusted with proton beam energy. In Syphers formulation this is described through a parameter of the S matrix elements, function of the nominal field B_0 in one of the helices [5]

$$\omega = \frac{(1 + G\gamma)B_0}{B\rho} \tag{2}$$

ω should remain constant at all $G\gamma$ in spite of the "1" in the numerator, that breaks the linearity of response [6].

The optimization of the snake field -for a field map- vs. $G\gamma$ has not been done yet. To emphasize the magnitude of the task, we should also recall that, because of saturation effects in the iron, field maps at high field are not identical to maps at low fields. The present calculations were performed by using a high field map, even for low field magnets, and using a field optimized for an intermediate value of $G\gamma$. A reasonable approach, at this stage of the analysis, is to parametrize the S matrix elements vs. beam energy. Accordingly, the calculation was repeated at energies corresponding to $\gamma = 25$ to 250. The result is shown in Fig. 11. A fitting, Fig. 12, using an expansion on base $s = \exp(-\gamma + \gamma_0)$

$$a = a_0 + A + B\,s + C\,s^2 \tag{3}$$

produced the coefficients shown in Table II

4. Orbit Matrices From a MO Map

T (orbit) matrices have been calculated from a MO map with *Snig*. A similar

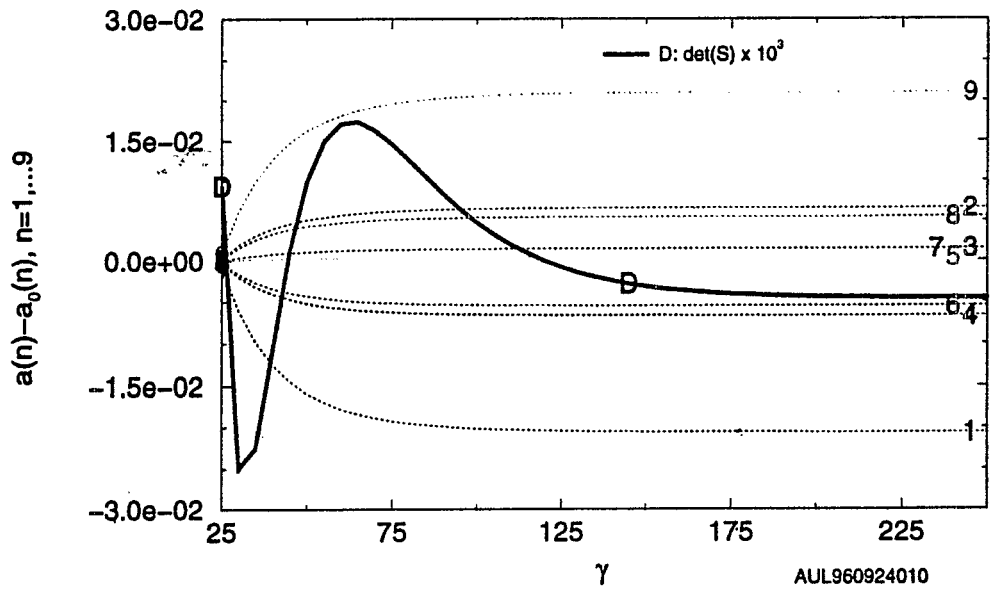

Figure 12: Snake S matrix coefficients vs. γ. MO map. fit.

Table II: Spin Matrices. Coefficients of the expansion in γ.

A	B	C
-6.642262684823E-3	2.689980719292E-3	3.706262987863E-3
4.448885965510E-4	-2.045166829963E-4	-2.256712197148E-4
-5.474359697490E-3	2.063815607736E-3	3.196530678736E-3
1.519896872518E-3	-8.310745332888E-4	-6.451036179242E-4
5.486581376952E-3	-2.090689651571E-3	-3.187264413617E-3
2.102177829034E-2	-8.816701580694E-3	-1.142642308771E-2

calculation and a trasformation up to third order has been already presented for a snake based on the BC field [13].

To calculate a T matrix, the technique was to track a certain number of particles by integration of the orbit equation. Particle initial coordinates were chosen at random with a gaussian distribution in all the components of $\vec{X}$ and particle energy. By solving a system of algebraic equations between the final and the initial coordinates of the same particles, a transformation expressed as a power expansion truncated to a pre established degree can be found. At the present stage of spin tracking, we are interested in a 0.th order 6×6 matrix, obtained by solving a system of linear equations. Since the center of the final beam will not in general coincide with the center of the initial beam in phase space, a minimum of $6 \times 6 + 6 = 42$ coefficients and then of representative particles will be needed. For more reliable results, we are constantly using a number of particles larger than 42, performing averages on the resulting matrices. Matrices thus built will represent to lowest order a true thick accelerator device, including its fringe field.

4.1. Symplectic Matrices

As already pointed out, a physical T matrix should be symplectic, otherwise the orbital motion is not calculated correctly in tracking. In particular, the beam emittance will grow. At constant beam energy, with only static magnetic fields, no space charge effects, and no chromaticity, the emittance and other integrals of the motions should remain constant. We recall than in a typical spin tracking run, a particle is followed for a number of turns than can exceed several 10^5, and then even a small error in the orbit symplecticity will cause a non acceptable emittance growth. The problem of emittance growth due to chromaticity of the helices will not be discussed here.

The code used, *Spink*, has been extensively described elsewhere [1]. It makes use of an integration routine based on the predictor-corrector Hamming HPC formalism with adjustable step. The routine starts with a 3.rd order Runge-Kutta, since HPC is not self-starting. The routine proved in the years to be very robust and quasi-symplectic. The limits of the sympecticity of the resulting matrices should be mostly attributed to the non perfect obeyance of the mapped field to Maxwell's equations.

Let us consider the problem in the transverse phase space (x, y). For a 0.th order transformation map, this requires that a matrix M satisfies the following condition (see e.g. [14])

$$M^T S M = S \tag{4}$$

where M^T is the transpose of M, and S is the matrix

$$S = \begin{pmatrix} 0 & 1 & 0 & 0 \\ -1 & 0 & 0 & 0 \\ 0 & 0 & 0 & 1 \\ 0 & 0 & -1 & 0 \end{pmatrix} \tag{5}$$

If Eq. (4) is satisfied, the matrix M corresponds to a rotation in phase space. Condition (4) is equivalent to the following six explicit relations between the matrix

elements

$$\begin{cases} (1122)+(3142)-1 & =0 \\ (1123)+(3143) & =0 \\ (1124)+(3144) & =0 \\ (1223)+(3243) & =0 \\ (1224)+(3244) & =0 \\ (1324)+(3344)-1 & =0 \\ det(M)-1 & =0 \end{cases} \tag{6}$$

with the definition

$$(ijkl) = M_{ij}M_{kl} - M_{il}M_{kj} \tag{7}$$

Note here that

$$\begin{cases} det_x = (1122) \\ det_y = (3344) \end{cases} \tag{8}$$

are the determinants of the 2×2 sub-matrices corresponding to the x and y planes.

A statistical definition of the transverse emittance of a beam, given the coordinates of the individual particles in phase space, is the determinant of the covariance matrix of the variables, position and transverse momentum

$$\epsilon^4 = det \begin{pmatrix} < x^2 > & < xx' > & < xy > & < xy' > \\ < x'x > & < x'^2 > & < x'y > & < x'y' > \\ < yx > & < yx' > & < y^2 > & < yy' > \\ < y'x > & < y'x' > & << y'y > & < y'^2 > \end{pmatrix} \tag{9}$$

where the dispersion of one of the variables is

$$\sigma^2 = \frac{1}{N}\sum(xi - < x >)^2 \tag{10}$$

and we have assumed in Eq. (9), for compact notation, that the averages, such as $< x >$ are $= 0$. If there is no coupling, the four dimension emittance is the product of the emittances in each transverse plane

$$\epsilon^2 = \epsilon_x \times \epsilon_y \tag{11}$$

The emittance in x is

$$\epsilon_x^2 = \langle (x - < x >)^2 \rangle \langle (x' - < x' >)^2 \rangle - \langle (x - < x >)(x' - < x' >) \rangle^2 \tag{12}$$

with a similar expression for ϵ_y^2.

It can be shown that if the matrix T is symplectic, the total emittance ϵ is conserved. If there is no coupling and $det(T) = 1$, the product $\epsilon_x \times \epsilon_y$ is conserved. Finally, with no coupling and $det_x = det_y = 1$, ϵ_x and ϵ_y are individually conserved.

By construction, analytical (Courant) helix matrices have a determinant exactly of 1 and are symplectic.

Matrices calculated from a field map in general aren't. This is a problem that would show up not only in our case, but also in machine optics codes like *Mad* [15],

that uses matrices obtained by truncation of some expansion. In *Mad*, the problem is solved by a transformation [16] that turns an approximately symplectic matrix into an exactly symplectic one. The argument runs as follow. Since a symplectic matrix M is a rotation, it can always be expressed in terms of a symmetric matrix W

$$M = (I + W)(I - W)^{-1} \tag{13}$$

with I the unitary matrix. We can invert and write W as a function of F. A quasi symplectic matrix $\tilde{M}$ yields a quasi symmetric $\tilde{W}$. Then, if we build the perfectly symmetric

$$W = \frac{1}{2}(\tilde{W} + \tilde{W}^T) \tag{14}$$

we can find the symplectic M using Eq. (13).

A second, direct method is based on the following observation. Since we can trace some of the problems of the lack of symplecticity to the non exact Maxwellian nature of the field we are using (see Appendix), and the errors in the *div* and *rot* equations are very small, it would take a very minor correction of the local field to produce a symplectic (i.e. physical) matrix. Besides, if we would measure the field instead of reading it from a calculated map, we would incur in measurements errors. The small modifications to the field values that will bring the field to satisfy Maxwell's to high accuracy are conceivably within these potential measuring errors. In conclusion, we can safely assume that we can doctor a little the orbit matrix, already almost symplectic, to complete symplect-ification.

The new matrix will be very close to the original, and it will allow us to track particles for many turns. Our doctoring was done by a numerical minimization by the Powell algorithm [12] of a function consisting of the sum of the squares of the terms in Eq. (6), with appropriate coefficients dictated by the function's derivatives.

A third strategy [17] is to make the field more Maxwellian, for instance by reading from the map only one field component and derive the others by using appropriate expansion coefficients. This method is more physically sound and should produce a more symplectic matrix. However, we expect that the integration of the equations of motion, as much symplectic as it may be, will introduce errors.

5. Calculation of Orbit Matrices

Results for T matrices in the MO maps are the following.

For the full snake, 256 particles were extracted at random on a gaussian distribution consistent with a beam emittance of 20 mm-mrad. Fig. 13 shows the envelope of some of the particles with the waist of the beam located at the center of the structure. Fig. 14 shows the phase (x, x') phase space at the entrance and at the exit of the snake. A linear fitting of the result produced the resulting matrix shown in Table III. In the table, the first column represents the coordinate of the 4 dimension phase space ellipsoid at the exit. The matrix is only approximately symplectic.

Table IV shows the results of the symplect-ization process by minimization, and the final values of the parameters of Eq. (6). The determinants of the symplectic matrix is almost three orders of magnitude smaller than for the original matrix. The values of the individual matrix elements are not very different from the original.

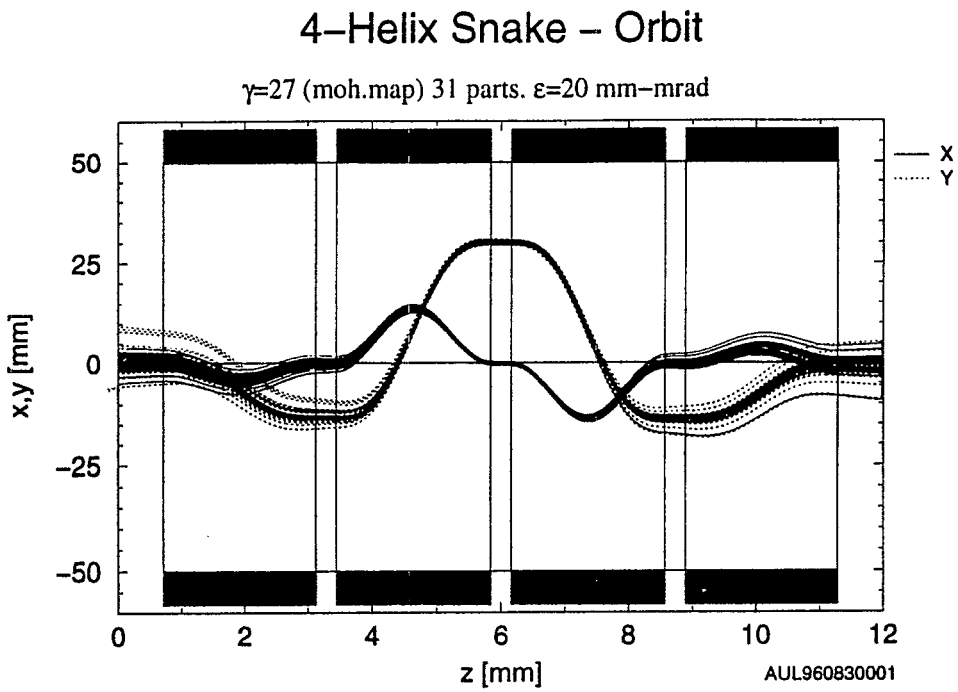

Figure 13: Envelope of trajectories for T matrix calculation in a snake.

Table III: T matrix for a snake (B=1.28953/4.18456).

0.9920306191376677	11.96006510061943	-5.1050749584865447E-3	-8.7880018951171750E-3
-1.3378539066999720E-3	0.9921174261971000	-5.2071548418545064E-5	3.4016820282902378E-3
3.3847654290992467E-3	2.2957362109107662E-2	0.9496547114988628	11.75579625614213
-8.8551634147480553E-5	-3.4007674143296486E-5	-8.3630160486648300E-3	0.9531749369129638

=> det$< T >$ = 1 +3.7303735145111094E-3

Table IV: T symplectic matrix. $\gamma = 27$

0.9911097266680854	11.94896268737290	-5.1003359665691278E-3	-8.7798440775944432E-3
-1.3366119898031406E-3	0.9911964531453604	-5.2023210901644815E-5	3.3985242796246884E-3
3.3816233839498041E-3	2.2936051010962195E-2	0.9487731561762228	11.74488346369663
-8.8469432518334769E-5	-3.3976105146914302E-5	-8.3552527414103572E-3	0.9522901137989749

=> Symplecticity parameters of Eq. (6)
=> det(T) = 1 +8.5469733879239840E-6

0.998357	-2.694776E-6	7.615925E-3
4.274411E-3	7.155221E-2	1.00162

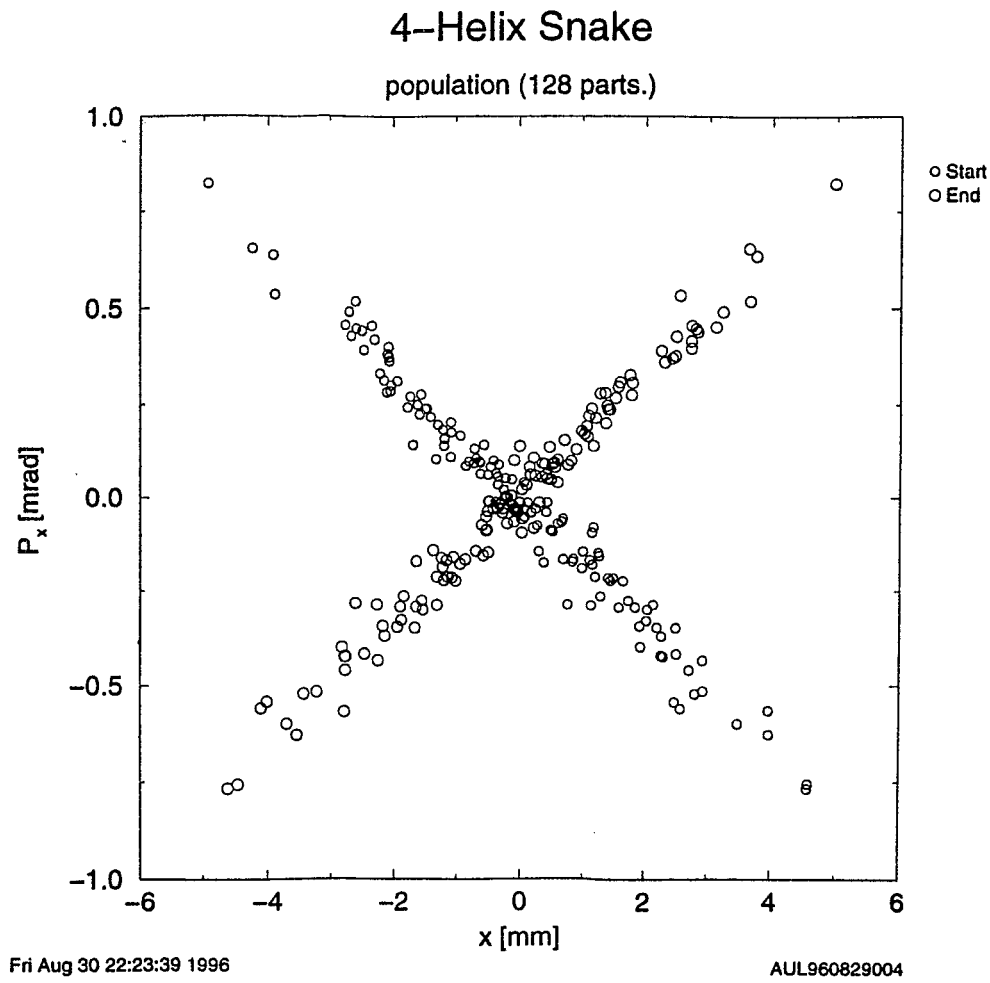

Figure 14: (x, x') phase space for T matrix calculation in a snake.

Table V: Emittance through a snake.

=> Entrance
partial emittances: ϵ_x, ϵ_y
$\pi\times$ 2.251109291171503E-5, 2.256254583135157E-5 m-rad
generalized emittance: ϵ
$\pi^2\times$ 5.030156671871370E-10 m^2rad^2
coupling: $\chi = \epsilon^2 - \epsilon_x \times \epsilon_y$
$\pi^2\times$ -4.891898347246872E-12 m^2rad^2
=> Exit. Symplectic matrix
partial emittances: ϵ_x, ϵ_y
$\pi\times$ 2.245841611004496E-5, 2.260296230399004E-5 m-rad
generalized emittance: ϵ
$\pi^2\times$ 5.030199664486383E-10 m^2rad^2
coupling: $\chi = \epsilon^2 - \epsilon_x \times \epsilon_y$
$\pi^2\times$ -4.606766294030711E-12 m^2rad^2

Table VI: Comparison of emittance growth.

	Entrance	Exit (Direct)	Exit (Symplectic)
ϵ_x	2.251109291171503E-5	2.250017010355032E-5	2.245841611004496E-5
$d\epsilon_x/\epsilon_x$		-4.852e-4	-2.333e-3
ϵ_y	2.256254583135157E-5	2.264498503331450E-5	2.260296230399004E-5
$d\epsilon_y/\epsilon_y$		3.654e-3	1.791e-3
ϵ	5.030156671871370E-10	5.048921035093790E-10	5.030199664486383E-10
$d\epsilon/\epsilon$		3.730e-3	8.546e-6
χ	-4.891898347246872E-12	-4.623911732548276E-12	-4.606766294030711E-12
$d\chi/\chi$		-5.478e-2	-5.829e-2

Table V shows the total emittance calculated from the particle distribution at the entrance and exit of the snake through the symplectic matrix. The total emittance is the determinant of the covariance matrix. Table VI shows how the emittance grows, in absolute and relative terms, if we use the Direct or the Symplectic matrix, respectively. The table shows that the total 4 dimensional emittance varies by two order of magnitude less with the symplect-ized matrix than with the direct matrix.

6. Appendix. MO Field Map and Maxwell Equations

In the MO field map, we checked how well satisfied are the two Maxwell equations

$$\begin{aligned} \nabla \cdot \mathbf{B} &= 0 \\ \nabla \times \mathbf{B} &= 0 \end{aligned} \tag{15}$$

We simply calculated the partial derivatives between two points separated by a distance dx, dy, or dz, as the field difference divided by the separation. We repeated the calculation in different regions of the helix, for different separation and employing an interpolation formula based on a 2^3 points (3-linear) or on 3^3 points (3-quadratic). Results are shown in Table VII for a separation of 1 mm between points, and quadratic

Table VII: Maxwell equations for a MO map.

3-quadratic interpolation	$dx = dy = dz = 1$ mm	
	Center	Near Edge
$\mathbf{P}$	(0.0000 0.0000 0.0000)	(0.0234 -0.0231 1.1000)
$\nabla \cdot \mathbf{B}$	-0.00257021 T/m	0.00349467 T/m
$(\nabla \times \mathbf{B})_z$	0.00085674 T/m	-0.00060580 T/m
$(\nabla \times \mathbf{B})_y$	-0.00035512 T/m	-0.00047360 T/m
$(\nabla \times \mathbf{B})_x$	0.00342675 T/m	-0.00330706 T/m

interpolation. We found a substantial improvement in moving from the linear to the quadratic interpolation. The table shows that the field is no more Maxwell-ian at the center of the helix than at both ends. Further work has shown that there is little or no gain to move to a cubic interpolation, and also that a smaller separation between points doesn't significantly change the values of the derivatives.

7. Acknowledgments

I gratefully acknowledge discussions on matrices and the symplecticity issue with Dr. H.Wu of Riken, Prof. T.Katayama of the University of Tokyo and Dr. I.Meshkov from Dubna and Eminent Scientist visiting Riken. I am also indebted with Dr. M. Ishihara and the Radiation Laboratory at Riken for their hospitality.

8. References

1. A.U.Luccio *Numerical Spin Tracking in a Synchrotron. Computer Code SPINK - Examples (RHIC).* Rept. BNL-52481, Upton, NY, September 1995. Also: Spin Note AGS/RHIC/SN No.011. Also: Proc. Adriatico Conf. Trieste, Italy, Dec. 1995.
2. V.I.Ptitsin and Yu.M.Shatunov, Proc 3.rd Workshop on Siberian Snakes (A.Luccio and T.Roser eds.) Upton, NY, Sept 12-13,1994, BNL-52453, p.15
3. J.P.Blewett and R.Chasman *Orbits and Fields in the Helical Wiggler.* J. Ap. Phys. 48 (1977) p.2692
4. E.D.Courant *Orbit Matrices for Helical Snakes.* AGS/RHIC/Spin Note No. 004, Upton, NY, November 8, 1994
5. M.J.Syphers *Spin Motion through Helical Dipole Magnets.* Spin Note AGS/RHIC/SN No 020, Upton, NY, February 1996.
6. L.D.Bozano Notes of Spin Seminar, Upton, NY, May 22,1996
7. *Tosca*, Vector Field Ltd., Oxford, UK
8. E.Willen and BNL Magnet Development Group, Private communication, 1996.
9. M.Okamura, T.Kawaguchi, T.Tominaka and T.Katayama *Three Dimensional Field Analysis of Helical Snake Magnets for RHIC.* Spin Note AGS/RHIC/SN No. 030, June 19, 1996 Also: Private Communication, Upton, NY, August 1996
10. A.U.Luccio *Numerical Studies of Siberian Snakes and Spin Rotators for RHIC.* BNL-52461, Upton, NY, April 1995. Also: Spin Note AGS/RHIC/S N No.

008. Also: Proc. Adriatico Conf. Trieste, Italy, Dec. 1995.
11. H.Wu, T.Katayama, K.Hatanaka, N.Saito and Y.Aoki *The Spin Tracking Study in RHIC for Polarized Proton.* Spin Note AGS/RHIC/SN No.026, April 29, 1996.
12. W.H.Press et al. *Numerical Recipes.* 2.nd ed. Cambridge University Press 1992
13. A.U.Luccio and F.Pilat, Proc. IEEE 1995 PAC, Dallas, TX, 5/1-5, 1995
14. M.Conte and W.T.McKay *An Introduction to the Physics of Particle Accelerators.* World Scientific, Singapore 1991
15. F.Ch.Iselin, *The Mad Program, Version 8.13. Physics Methods Manual.* CERN/SL/(2(AP), Geneva, January 10, 1994
16. L.H.Healy, *Lie Algebraic Methods for Treating Lattice Parameter Errors in Particle Accelerators.* PhD Thesis, University of Maryland, 1986
17. T.Katayama *Multipole Field Expansion of Helical Magnet.* Riken Spin Note, September 1996